## Title

Hollow Micropillar Array Method for High-Capacity Drug Screening on Filter-Grown Epithelial Cells



## Journal

Analytical Chemistry, 90(12)

## ISSN

0003-2700

## Authors

Jin, Byung-Ju
Lee, Sujin
Verkman, Alan S

## Publication Date

2018-06-19

## DOI

10.1021/acs.analchem.8b01554

Peer reviewed

HHS Public Access

Author manuscript

*Anal Chem*. Author manuscript; available in PMC 2019 April 12.

Published in final edited form as:

*Anal Chem*. 2018 June 19; 90(12): 7675–7681. doi:10.1021/acs.analchem.8b01554.

# Hollow Micropillar Array Method for High-Capacity Drug Screening on Filter-Grown Epithelial Cells

**Byung-Ju Jin**, **Sujin Lee**, and **Alan S. Verkman***

Departments of Medicine and Physiology, University of California, San Francisco, California 94143-0521, United States

## Abstract

New high-throughput assay formats and innovative screening technologies are needed for miniaturized screens using small quantities of near-native, patient-derived cells. Here, we developed a hollow micropillar array method to screen compounds using epithelial cells cultured on a porous support, with the goal of screening thousands of compounds using a single 24 mm diameter transwell filter containing cultured cells. Test compounds (~1 nL) in an alginate hydrogel were printed by microinjection in hollow cylindrical micropillars (height = 150 $\mu$m, inner diameter = 100 $\mu$m) spaced 300 $\mu$m apart in a square array configuration. Compounds were delivered by positioning the array near the surface of a cell layer, with 5–10 $\mu$m of distance between the micropillars and cell surface. Micropillar array geometry, and the viscosity of the hydrogel and overlying solutions, were optimized computationally and experimentally to produce sustained exposure of cells to test compounds with minimal cross-talk from compounds in neighboring micropillar wells. The method was implemented using a 10 × 10 micropillar array (size = 3 × 3 mm) on CFTR-expressing epithelial cells, in which CFTR chloride channel function was measured from fluorescence in response to iodide addition using a genetically encoded cytoplasmic yellow fluorescent protein halide indicator. The hollow micropillar array platform developed here should be generally applicable for high-capacity drug screening using small numbers of cells cultured on solid or porous supports.

## Graphical Abstract

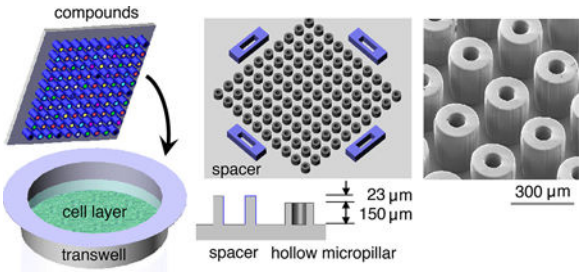


***Corresponding Author** Mailing Address: Alan S. Verkman, M.D., Ph.D., University of California, 1246 Health Sciences East Tower, San Francisco, CA 94143-0521, United States; Phone: 415 476-8530; Fax: 415 665-3847; Alan.Verkman@ucsf.edu.

Notes

The authors declare no competing financial interest.

Miniaturized high-throughput screening is needed in the pharmaceutical industry to accelerate drug discovery and reduce costs and to advance personalized medicine utilizing limited quantities of patient-derived cells.[1–4] One example is cystic fibrosis, in which loss-of-function mutations in the cystic fibrosis transmembrane conductance regulator (CFTR) chloride channel cause lung and gastrointestinal disease by impairment of epithelial fluid transport. Screens for modulators of mutant CFTRs utilizing transfected heterologous cells have produced compounds of limited efficacy, such as correctors of defective CFTR-ΔF508 cellular processing (reviewed in refs [5–7]). It has become apparent that compounds identified from screens done on transfected cells may not translate to primary, differentiated cultures of human cystic fibrosis airway cells grown on porous supports under native, air–liquid interface conditions.[8] There is a need to develop screening methods utilizing primary, near-native patient-derived cystic fibrosis cells, which are generally limited in amount.

Limited progress has been made in high-capacity microarray screening methods using microdispenser technology. The general approach has been fabrication of confined microwells, in which compounds are printed in separate wells or on pillars.[9–12] However, these methods are at an early stage, with major challenges including well density, alignment of micropillars with wells, and cell culture in microwells. Of relevance to the goal herein, microwell methods are not suitable for epithelial cells cultured on porous filters at an air–liquid interface. In early proof-of-concept work, a method was reported for cell exposure to test drugs, in which a glass plate containing printed compounds is contacted with a cell culture.[13,14] Challenges with this approach, however, include cross-talk of neighboring compounds, knowledge of the exact compound concentrations being exposed to cells, and the mechanics of making reliable contact between the glass plate containing test compound and the cell culture. No approach has yet been developed for filter-grown epithelial cells, as needed in cystic fibrosis drug discovery.

Here, we report a simple and practical high-capacity screening platform, which builds on the early work cited above,[13,14] that can be applied to cells grown on solid supports such as plastic or on porous filters. The approach, as diagrammed in Figure 1A, is printing of compounds in a hydrogel in a dense square array of hollow cylindrical micropillars that make close contact with the apical-facing surface of an epithelial cell monolayer. Micropillar and contact geometry, and solution viscosities, were chosen to produce sustained local exposure of cells to test compounds with minimal cross-talk from compounds in neighboring micropillars. Proof-of-concept studies were done using a small square array of 100 micropillars on filter-grown CFTR-expressing epithelial cells.

## METHODS

### Fabrication of Hollow Micropillar Arrays.

A hollow micropillar array was fabricated to print 100 compounds in a 3 × 3 $mm^2$ area, in which four ~23 $\mu$m high rectangular spacers were fabricated to set an ~10 $\mu$m gap between the upper surface of micropillars and the cell layer (assuming ~13 $\mu$m cell height). The hollow micropillar array was fabricated using conventional double layer soft-lithography, as diagrammed and detailed in Supplementary Figure S1. The first layer, with ~23 $\mu$m thickness, was fabricated using an SU-8 2015 photoresist (MicroChem, Westborough, MA)

on a 4 in. wafer as per manufacturer's instructions. The second layer of ~150 μm height containing the hollow micropillar array was fabricated by spin-coating an SU-8 2100 photoresist (MicroChem) on the first layer. The PDMS replica of the micropillar array was molded using Sylgard 184 base material and curing agent with a 10:1 ratio. Figure 1B (right) shows a scanning electron micrograph of the fabricated hollow micropillar wells.

The structured PDMS layer was treated with air plasma (PlasmaFlo PDC-FMG and Plasma Cleaner, PDC-32G Harrick Plasma, Ithaca, NY) at 700 mTorr for 90 min. Just after the plasma treatment, the PDMS layer was submerged in a polyethylene glycol (PEG) solution (molecular weight = 200, Sigma-Aldrich, St. Louis, MO), and the PDMS surface was coated for 30 min to make a hydrophilic surface to facilitate compound printing in the hollow micropillars. The PEG-coated PDMS channel was washed with deionized water and dried with $N_2$ gas for 1 h at room temperature. The PEG coating quality was confirmed by measuring the contact angle on the PDMS surface, which were ~110° and ~20° for untreated PDMS and PEG-coated PDMS, respectively.

### Compound Microprinting.

Compounds (~1 nL volume) in an alginate solution (alginic acid sodium salt from brown algae, Sigma-Aldrich) were printed in each hollow micropillar well using microdispensing technology (sciFLEXARRAYER S3, Scienion, Berlin, Germany). First, 1 nL of 0.2% $CaCl_2$ was printed in each well and dried completely for 30 min at room temperature. Then, 1 nL of a 1% alginate solution containing 25 μM test compound (from DMSO stock) was microdispensed in the hollow micropillar well, with a final DMSO concentration of 5%. The test compound/alginate mixture gelled within a few minutes. After printing, the hollow pillar array was kept in a humidified chamber (tape-sealed Petri dish lined with water-soaked tissue paper) to prevent drying.

### Mathematical Modeling of Compound Diffusion.

Cross-talk was analyzed by mathematical modeling of compound diffusion using Comsol Multiphysics (version 3.4; Comsol Inc., Burlington, MA). Compound diffusion in the three-dimensional hollow micropillar array is described by the diffusion equation

$$\partial C/\partial t = -D\nabla^2 C \quad (1)$$

where $C$ is compound concentration, $t$ is the time, and $D$ is compound diffusion coefficient. The computational domain was a 6 mm diameter disk with 160 μm in height containing a 5 × 5 hollow micropillar array (Figure 2A). Micropillars were 100 μm in diameter and 150 μm in height, with a 300 μm gap between micropillars. Different distances between the micropillar upper surface and the cell layer were modeled (2, 5, 10, 20, 50, and 100 μm) (Supplementary Figure S2).

As the initial condition, the cylindrical hollow micropillar well contained uniformly distributed test compound (concentration = $C_{well}$), with zero concentration elsewhere. Compound diffusion coefficient ($D$), which is related to solution viscosity by the Stokes–

Einstein equation, $D = k_B T/(6\pi\eta r)$, was varied between $10^{-9}$ and $10^{-11}$ $m^2/s$, corresponding to diffusion in water (1 cP) and a viscous 100 cP solution. Impermeant boundary conditions were applied at the hollow micropillar surface and the cell layer, and a nonreflective boundary condition was applied at the outer boundary.

### Fluorescent Dye Diffusion Measurements.

For testing diffusion, a polar fluorescent dye (10 μM sulforhodamine 101, 607 Da, Sigma-Aldrich) was printed together with test compounds (in alginate hydrogel) in a subset of microwells. Dye diffusion following array attachment to a glass plate or cell layer was measured by fluorescence confocal microscopy using a 4× lens.

### Drug Release from Alginate Hydrogels.

Drug release from alginate hydrogels was determined using high-performance liquid chromatography–mass spectrometry (LC/MS). First, 20 μL of 0.2% $CaCl_2$ was added in a 96-well plate, dried, and a 10 μM concentration of drug in 20 μL of 1% alginate solution was added into the $CaCl_2$-containing wells. After alginate gelation, 200 μL of PBS was added on top of the gel at room temperature, and at specified times, the PBS overlying solution was collected, mixed with 500 μL of ethyl acetate, and centrifuged for 15 min at 3000 rpm. The organic layer was used for LC/MS analysis. HPLC was done on a Xterra MS C18 column (2.1 mm × 100 mm, 3.5 μm) with 0.2 mL/min of water/acetonitrile (containing 0.1% formic acid), 25 min linear gradient, 5–95% acetonitrile. For each drug, a parallel standard curve was generated, in which integrated peaks were compared with calibration standards that were processed identically to test samples.

### Iodide Transport in CFTR-Expressing FRT Cells.

FRT cells stably expressing human wildtype CFTR and yellow fluorescent protein YFP-H148/I152L were cultured on polyester transwell filters until they formed a tight monolayer (electrical resistance > 3 kOhm·$cm^2$), as described.[15,16] The cell culture medium was then replaced with a viscous solution consisting of 2% methylcellulose (~41 000 Da, Sigma-Aldrich) in PBS. The cell layer was contacted with a 10 × 10 micropillar array for 10 min, and then, the viscous solution was rinsed. For transport measurement, an $I^-$-containing solution (PBS with 120 mM chloride replaced by $I^-$) was added manually on top of the cell layer. YFP fluorescence of the entire cell culture area was monitored for 5 min at 10 Hz using a 2× magnification lens (CFI Plan Apo Lambda 2X, Nikon, Melville, NY) with an EMCCD camera detector (C9100, Hamamatsu). YFP fluorescence is reduced as the added extracellular $I^-$ is transported into cell cytoplasm through activated CFTR. The time course of fluorescence for each of the 100 locations, each integrated over the 100 μm diameter circular cell area overlying the corresponding micropillar well, was determined using ImageJ. A specified subset of hollow micropillars contained the CFTR agonist forskolin (10 μM in alginate hydrogel).

# RESULTS

## Design of Hollow Micropillar Array.

The design criteria for the hollow micropillar array included feasibility of fabrication and a high micropillar density enabling exposure of cells in the vicinity of micropillars to a sustained concentration of test compound with minimal cross-talk from compounds in neighboring wells. Also, there should be no direct contact between the micropillars and cell layer to avoid cell injury. In addition to challenges in specifying micropillar geometry and density to accomplish these goals was the need to establish a hydrogel vehicle and a PDMS treatment to stably retain and release compounds from the hollow micropillars.

A hollow micropillar array was designed to print ~2500 compounds in an ~1.5 × 1.5 $cm^2$ area (Figure 1A, left), which would allow testing of ~5000 compounds on a standard 24 mm diameter porous filter containing a monolayer of cultured cells.

The dense micropillar array consisted of 100 $\mu$m inner diameter cylindrical hollow micropillars spaced 300 $\mu$m apart (Figure 1A right) so that ~20 cells of typical size would overlie the hollow area of each micropillar. Compounds are dispensed in the hollow cylindrical volume of micropillars. For initial design optimization, various hollow micropillar designs (inner diameters: 100, 150, and 200 $\mu$m, with different heights) were tested for feasibility of fabrication and compound printing and modeled computationally to confirm compound exposure to cells with minimal cross-talk.

Following design optimization as described below, the hollow micropillar array used herein was fabricated to print 100 compounds in a 3 × 3 $mm^2$ area (Figure 1B, left), in which a 23 $\mu$m spacer was fabricated to set an ~10 $\mu$m gap between the upper surface of micropillars and the cell layer. A scanning electron micrograph of the fabricated hollow micropillar array (Figure 1B, right) shows the cylindrical wells in each micropillar and a rectangular spacer (figure inset, upper left).

## Computational Modeling of Hollow Micropillar Array.

An important design criterion for high-capacity compound screening was maximizing the number of compounds screened per area of cell culture with minimal cross-talk from compound in neighboring micropillars. A typical small molecule with diffusion coefficient ($D \approx 10^{-9}$ $m^2/s$) diffuses ~1.5 mm during a 10 min incubation according to simple theoretical analysis $x \approx (4Dt)^{1/2}$, where $x$ is diffusion distance, and $t$ is diffusion time.

Two approaches were implemented in order to minimize cross-talk and increase compound array density: (i) increased viscosity of solution overlying cells; and (ii) a hollow pillar microstructure. Increased solution viscosity reduces the

compound diffusion coefficient according to the Stokes–Einstein equation, $D = k_B T/(6\pi\eta r)$, where $D$ is diffusion coefficient, $k_B$ is Boltzmann's constant, $T$ is absolute temperature, $\eta$ is solution viscosity, and $r$ is the particle radius. Solution viscosity is increased experimentally using methyl-cellulose. A hollow micropillar geometry provides a reservoir to contain test

compounds and reduces cross-talk because of compound dilution into the space between neighboring micropillars.

We characterized the hollow micropillar design by finite-element diffusion simulations. Figure 2A shows the computational geometry, with the same dimensions as the fabricated hollow micropillar array (see Methods for details). Compound exposure to cells and cross-talk between neighboring compounds was analyzed for different solution viscosities and micropillar heights. Figure 2B (left) shows pseudo-color images of compound concentration with overlying solutions of relative viscosities of 1 and 100 cP. Rapid compound diffusion was found for $\eta = 1$ cP, with compound seen in neighboring spots by 5 min; however, compound was not seen in the neighboring spots for $\eta = 100$ cP. These observations are confirmed in concentration line scans in Figure 2B (right). Figure 2C (left) shows relative compound concentration at the cell surface in the circular region of the central micropillar normalized to the original compound concentration in the micropillar well. Compound concentration at the cell surface remained high for at least 10 min for $\eta = 100$ cP and for lesser times with lower $\eta$. Compound exposure was reduced, as expected, with increasing gap distance between the cell surface and the hollow micropillar (Supplementary Figure S2). Additional computational modeling (Supplementary Figures S3 and S4) of compound release from hollow micropillars was done for various combinations of microwell and outside solution viscosities, showing the expected slowed compound release with increased viscosity of the outside solution or of the alginate-containing well.

Cross-talk was analyzed by computing compound concentration at the cell surface in the region of the central micropillar and at a neighboring spot. The time-integrated concentration at the neighboring spot ($\int C\mathrm{d}t$ at $x = 300$ $\mu$m) was normalized to that of the central spot ($\int C\mathrm{d}t$ at $x = 0$ $\mu$m). Figure 2C (right) shows little or no cross-talk in 10 min for $\eta = 10$ or 100 cP. Additional computations (not shown) investigated micropillar height and gap distance between the micropillars and the cell surface. Reduced micropillar height reduced compound exposure (because of reduced compound amount) and increased cross-talk (because of reduced volume between micropillars). Compound exposure and cross-talk were relatively insensitive to a 2-fold change in gap distance. The fabricated hollow micropillar array was designed with ~10 $\mu$m gap distance between the upper surface of micropillars and the cell layer.

## Compound Formulation and Microdispensing.

Compounds were dispensed in the hollow micropillar wells in a total 1 nL volume using microdispensing technology as described in the Methods. Following testing of different hydrogel materials (see Discussion), we found that an alginate hydrogel was suitable for the application herein. Alginate solutions remain liquid prior to contacting $CaCl_2$. For microdispensing, $CaCl_2$ was first dispensed, dried, and then, compounds in a 1% alginate solution were dispensed. Testing of different compound solubilizing agents (e.g., dimethyl sulfoxide, DMSO; dimethylacetone, DMA) showed that DMSO up to 30% vol/vol did not interfere with alginate gelation and that compounds remained solubilized down to 5% vol/vol DMSO. Confocal microscopy using rhodamine 101 as test compound indicated that microdispensing produced uniform fluorescence throughout microwells, with fluorescence

seen up to the top of each microwell (not shown). After microdispensing, storage of micropillar arrays in a humidified chamber prevented significant evaporation for at least several days.

To test the efficiency of compound release from alginate hydrogels, the release was tested of five commonly prescribed drugs with a wide range of *c*log*P*, which represents the compound octanol/water partition coefficient and hence a measure of hydrophilicity, from 0.91 (acetaminophen) to 5.3 (atorvastatin). Drugs were held in alginate hydrogels as done for test compounds in a screening application, and release into an overlying PBS solution at 3 h was quantified by LC/MS (Figure 3A). The percentage of drug release was determined from the measured amount of drug in the overlying solution compared with that expected for 100% drug release (accounting for relative volumes of hydrogel and overlying solution). Figure 3B shows near-complete release of four out of the five randomly chosen drugs tested, indicating reversible drug dissolution in the alginate hydrogel with minimal absorption into the PDMS substrate. The reason(s) for reduced apparent release of metformin are not known. For one of the drugs (atorvastatin), the kinetics of release was quantified by assaying sampled fluid at different times. Figure 3C shows that atorvastatin release from the hydrogel occurred with a half-time of ~10 min, which is consistent with the expected time for its diffusion out of the cylindrical micropillar well.

### Release and Diffusion of a Fluorescent Dye from Hollow Microfibers.

As experimental validation of the computational modeling, alginate was microdispensed into a 10 × 10 array of hollow microfibers with rhodamine 101 added to a subset of micropillars (Figure 4A,B). Figure 4C shows rhodamine 101 diffusion from the micropillar wells, as measured by confocal microscopy. Less than 2% of rhodamine 101 fluorescence was seen in neighboring wells at 10 min following addition of a 100 cP solution, confirming the absence of significant cross-talk.

### CFTR Activation Measurement on Filter-Grown Epithelial Cells.

As an example to demonstrate the utility of the hollow micropillar array design, CFTR activation was measured in FRT epithelial cells expressing human CFTR and a yellow fluorescent protein (YFP) cytoplasmic halide sensor. The cells were cultured on a porous transwell filter. As diagrammed in Figure 5A, following extracellular $I^-$ addition, CFTR activation by the cAMP agonist forskolin allows $I^-$ entry into cells and consequent quenching of cytoplasmic YFP fluorescence.

A 10 × 10 hollow micropillar array, as used in validation studies described above, was loaded with alginate hydrogels, some of which contained 10 $\mu$M forskolin (Figure 5B, left). After contacting the cell layer for 10 min, the overlying solution was exchanged to an $I^-$-containing solution. A YFP fluorescence image taken at 10 min (Figure 5B, right) shows reduced fluorescence in cells overlying (and nearby) forskolin-loaded micropillars. Figure 5C shows deduced kinetics of fluorescence quenching following $I^-$ addition, in which the fluorescence signal was integrated over 100 $\mu$m circles in cells overlying forskolin-containing micropillars (“+forskolin”, four examples shown) and a neighboring area of cells (“−forskolin”). Forskolin activation of CFTR increased the initial curve slope by >14-fold,

with full-field analysis giving a robust assay statistical *Z*-factor > 0.65, indicating the ability to identify activators with a high level of confidence.

## DISCUSSION

The results herein provide proof-of-concept for a high-capacity drug screening approach involving compound release from hydrogels printed in cylindrical microwells in close contact with a monolayer cell culture. The hollow micropillar array design with hydrogel-embedded compounds and viscous aqueous solution between the micropillars and cell layer satisfied the specified screening criteria, which included exposure of cells to test compound for up to tens of minutes with minimal cross-talk, and efficient compound retention and release from hydrogels. Specification of the various parameters, including micropillar geometry and density as well as hydrogel composition and solution viscosity, involved trade-offs between compound density, cell exposure time to test compounds, and cross-talk from compounds in neighboring wells. Varying of the parameters, for example, increasing solution viscosity and reducing micropillar diameter, would allow for a substantially increased compound density; however, from experience, practical considerations of fabrication and microprinting would preclude much more than an ~5-fold increase in micropillar density. The computational modeling presented in Figure 2 and Supplementary Figures S2–S4 shows the predicted interplay among the parameters with regard to compound exposure and cross-talk and provides justification for the parameter selection herein. An important design feature, as modeled mathematically and validated experimentally, was the hollow, long micropillar design, which allowed retention of adequate compound amounts for sustained release and slowed lateral diffusion of compounds following their release.

Poly(dimethylsiloxane) (PDMS) is the most popular polymeric material used in microfluidics for biological and pharmaceutical applications due to its favorable characteristics, including lack of toxicity, biocompatibility, ease of handling, and low cost.[17] While convenient in manufacturing, PDMS can absorb small molecules such as drugs,[18] and the hydrophobic PDMS surface can entrap air bubbles, which in the design here could impair fluid contact between the micropillars and cell layer. Various approaches have been reported to coat PDMS to create a hydrophilic surface to prevent small molecule absorption.[19–21] Here, we used a PEG-200 coating, which was technically simple and prevented compound absorption and air bubbles. PEG has been shown to produce stable, long-term PDMS surface modification.[22–24]

For compound retention in the cylindrical hollow micropillars, compounds were printed in an alginate hydrogel, which prevented compound precipitation and allowed compound release, and was easy to handle in that gelation occurred only upon contact with a predeposited calcium salt. A hydrogel of some type is needed to provide a mechanical framework for compound retention, as free-flowing aqueous solutions are easily disturbed during handling of the micropillar array. Alginate is a natural polysaccharide derived from brown algae and is considered an attractive biomaterial for biomedical applications.[25] Small molecule diffusion in alginate hydrogels is similar to their diffusion in the surrounding aqueous medium,[26] as the alginate only comprises a small volume fraction, and small

molecules are substantially smaller (≪1 nm) than the alginate pore size (5–16 nm).[27,28] Various alternative hydrogels have been used for drug delivery such as poly(ethylene glycol) diacrylate (PEGDA) and poly($_D$),($_L$)-lactide/glycolide copolymer (PLGA);[12,13] however, compound release in these polymers occurs over hours or days, which is not suitable for screening work here, in which release over minutes is needed. Agarose and Matrigel are not easily adapted for dispensing multiple compounds between of their rapid gelation and hence clogging of microneedles. The alginate hydrogel used here, with controlled calcium-dependent gelation, provided a stable vehicle to retain test compounds and release them into an overlying solution when needed.

Limitations of the approach described herein are noted, as well as further optimization and refinements. The shelf life of compound-loaded micropillar arrays was not determined as the arrays were used within a week of their microprinting. For commercial distribution, a shelf life of months would be desirable. The time of exposure of cells to test compounds released from the hollow micropillars, which was tens of minutes for parameters used here, could be extended by increasing solution viscosity and compound concentration, through probably not easily more than a few hours, as would be desirable, for example, in CFTR corrector drug screening. Some variability was seen in drug release from hydrogels, suggesting that certain compounds may not be compatible with alginate hydrogels, which requires further investigation and perhaps the need to include additional solvating substances in the hydrogel. Finally, the proof-of-concept study of CFTR activation here involved manual separation of the micropillar array from the cell layer, followed by manual solution addition. These assay steps are suitable for automation, perhaps using a perfusion system to wash away test compounds and add assay initiators.

## CONCLUSION

Though the application demonstrated here was the measurement of CFTR activation in epithelial cells cultured on a porous filter, the hollow micropillar array approach is generalizable to cell monolayers of any type grown on solid or porous supports and to kinetic or steady-state read-out of an optical signal for any enzyme, transporter, receptor or other target, or a cell phenotype. For example, assays of ion channels and solute transporters are possible using suitable fluorescent indicators of $Na^+$, $K^+$, $Cl^-$, pH, membrane potential, and others. Other possible read-outs include optical imaging cell shape and motility. The micropillar approach developed here is also particularly useful for screening assays utilizing limited quantity of cells, as in personalized *n*-of-1 studies using patient-derived primary cells and in assays utilizing limited quantities of test drugs.

## Supplementary Material

Refer to Web version on PubMed Central for supplementary material.

## ACKNOWLEDGMENTS

This work was supported by National Institutes of Health grants DK72517, DK099803, DK075302, DK101373, EB00415, and EY13574, and grants from Emily's Entourage and the Cystic Fibrosis Foundation.

## REFERENCES


(1). Mayr LM; Bojanic D Curr. Opin. Pharmacol 2009, 9, 580–588. [PubMed: 19775937]

(2). Cheong R; Paliwal S; Levchenko A Expert Opin. Drug Discovery 2010, 5, 715–720.

(3). Bellomo F; Medina DL; De Leo E; Panarella A; Emma F J. Inherited Metab. Dis 2017, 40, 601–607. [PubMed: 28593466]

(4). Nickischer D; Elkin L; Cloutier N; O'Connell J; Banks M; Weston A Methods Mol. Biol 2018, 1683, 165–191. [PubMed: 29082493]

(5). Hanrahan JW; Matthes E; Carlile G; Thomas DY Curr. Opin. Pharmacol 2017, 34, 105–111. [PubMed: 29080476]

(6). Mijnders M; Kleizen B; Braakman I Curr. Opin. Pharmacol 2017, 34, 83–90. [PubMed: 29055231]

(7). Li H; Pesce E; Sheppard DN; Singh AK; Pedemonte N J. Cystic Fibrosis 2018, 17, S14.

(8). Pedemonte N; Tomati V; Sondo E; Galietta LJ Am. J. Physiol. Cell Physiol 2010, 298, C866–C874. [PubMed: 20053923]

(9). Kwon CH; Wheeldon I; Kachouie NN; Lee SH; Bae H; Sant S; Fukuda J; Kang JW; Khademhosseini A Anal. Chem 2011, 83, 4118–4125. [PubMed: 21476591]

(10). Lee DW; Choi Y-S; Seo YJ; Lee M-Y; Jeon SY; Ku B; Kim S; Yi SH; Nam D-H Anal. Chem 2014, 86, 535–542. [PubMed: 24199994]

(11). Ding Y; Li J; Xiao W; Xiao K; Lee J; Bhardwaj U; Zhu Z; Digiglio P; Yang G; Lam KS; Pan T Anal. Chem 2015, 87, 10166–10171. [PubMed: 26334956]

(12). Fujita S; Onuki-Nagasaki R; Ikuta K; Hara Y Biofabrication 2017, 9, 011001.

(13). Bailey SN; Sabatini DM; Stockwell BR Proc. Natl. Acad. Sci. U. S. A 2004, 101 (46), 16144–16149. [PubMed: 15534212]

(14). Jin BJ; Ko EA; Namkung W; Verkman AS Lab Chip 2013, 13, 3862–3867. [PubMed: 23907501]

(15). Lee M-Y; Park CB; Dordick JS; Clark DS Proc. Natl. Acad. Sci. U. S. A 2005, 102, 983–987. [PubMed: 15657119]

(16). Cil O; Phuan PW; Lee S; Tan J; Haggie PM; Levin MH; Sun L; Thiagarajah JR; Ma T; Verkman AS Cell. Mol. Gastroentrol. Hepatol 2016, 2, 317–327.

(17). Whitesides GM; Ostuni E; Takayama S; Jiang X; Ingber DE Annu. Rev. Biomed. Eng 2001, 3, 335–373. [PubMed: 11447067]

(18). Van Meer BJ; De Vries H; Firth KSA; Van Weerd J; Tertoolen LJG; Karperien HBJ; Jonkheijm P; Denning C; Ijzerman AP; Mummery CL Biochem. Biophys. Res. Commun 2017, 482, 323–328. [PubMed: 27856254]

(19). Hellmich W; Regtmeier J; Duong TT; Ros R; Anselmetti D; Ros A Langmuir 2005, 21, 7551–7557. [PubMed: 16042494]

(20). Huang B; Wu H; Kim S; Zare RN Lab Chip 2005, 5, 1005–1007. [PubMed: 16175253]

(21). Wang JD; Douville NJ; Takayama S; Elsayed M Ann. Biomed. Eng 2012, 40, 1862–1873. [PubMed: 22484830]

(22). Lillehoj PB; Wei F; Ho C-M Lab Chip 2010, 10, 2265–2270. [PubMed: 20596556]

(23). Lillehoj PB; Ho C-M A long-term, stable hydrophilic poly(dimethylsiloxane) coating for capillary-based pumping. Proceedings of the IEEE 23rd International Conference on Micro Electro Mechanical Systems (MEMS), 2010, 1063–1066; https://scholars.opb.msu.edu/en/publications/a-long-term-stable-hydrophilic-polydimethylsiloxane-coating-for-c-4.

(24). Demming S; Lesche C; Schmolke H; Klages C-P; Buttgenbach S Phys. Status Solidi A 2011, 208, 1301–1307.

(25). Alvarez-Lorenzo C; Blanco-Fernandez B; Puga AM; Concheiro A Adv. Drug Delivery Rev 2013, 65, 1148–1171.

(26). Tanaka H; Matsumura M; Veliky IA Biotechnol. Bioeng 1984, 26, 53–58. [PubMed: 18551586]

(27). Mazutis L; Vasiliauskas R; Weitz DA Macromol. Biosci 2015, 15, 1641–1646. [PubMed: 26198619]

(28). Lee KY; Mooney DJ Prog. Polym. Sci 2012, 37, 106–126. [PubMed: 22125349]

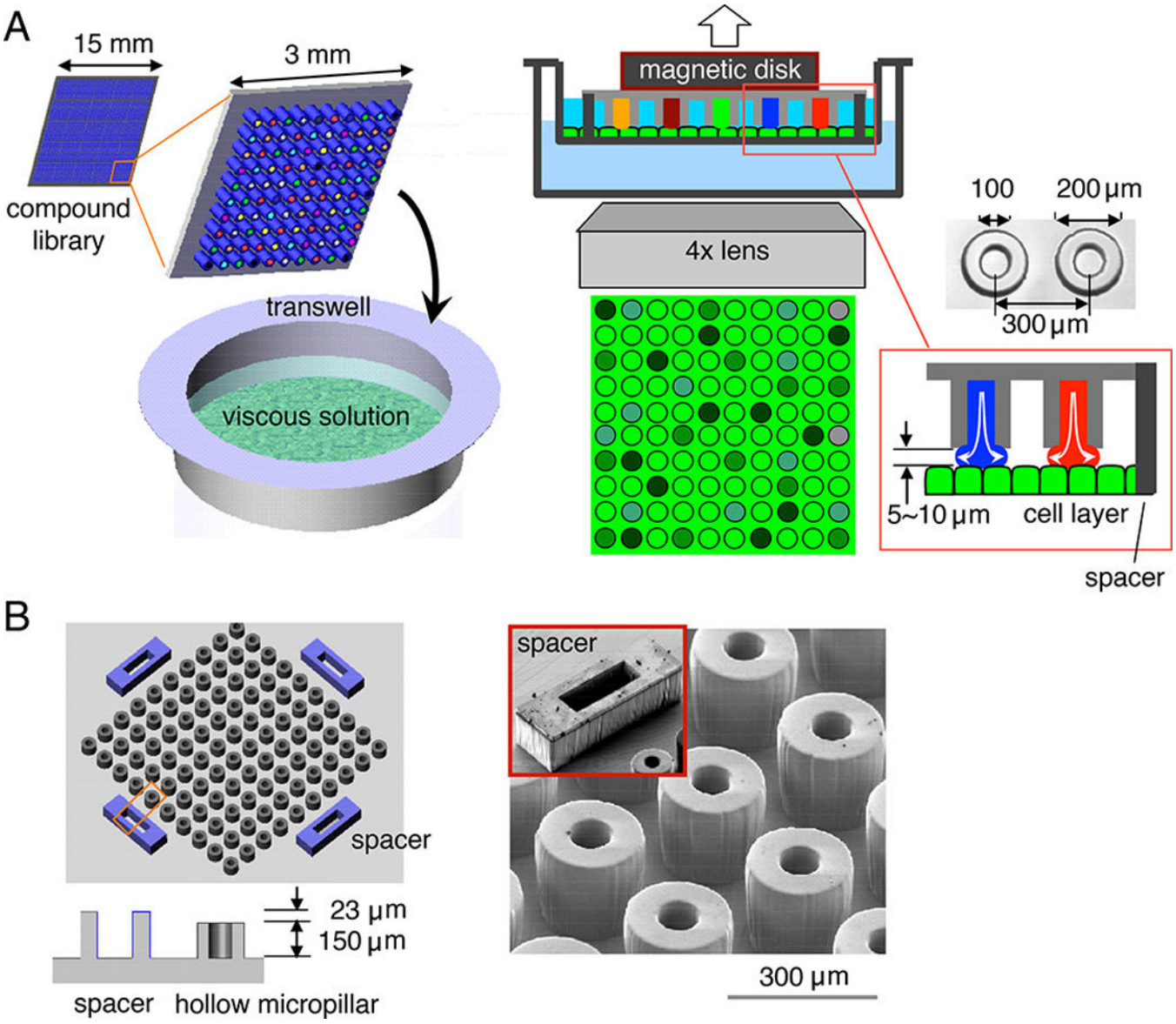


**Figure 1.**

Hollow micropillar array to deliver compounds for high-capacity drug screening. (A) (left) Principle of method. Compounds in an alginate hydrogel are microprinted in hollow cylindrical micropillars. The PDMS hollow micropillar array is contacted with a cell monolayer for tens of minutes to deliver compounds to cells overlying the hollow micropillars. Micropillar geometry and the viscosity of the surrounding solution were optimized for sustained compound delivery with minimal cross-talk from compounds in neighboring micropillars. (right) Schematic showing compound release from hollow micropillars. Following compound incubation, the micropillar array is separated from the cell layer and a fluorescence-based assay is initiated, in which compound identity is determined from cell position. (B) (left) 10 × 10 hollow micropillar array fabricated for studies herein, showing hollow micropillars and rectangular spacers to set gap between

micropillars and the cell layer. (right) Scanning electron micrograph of micropillar array, with hollow rectangular spacer shown in the inset.

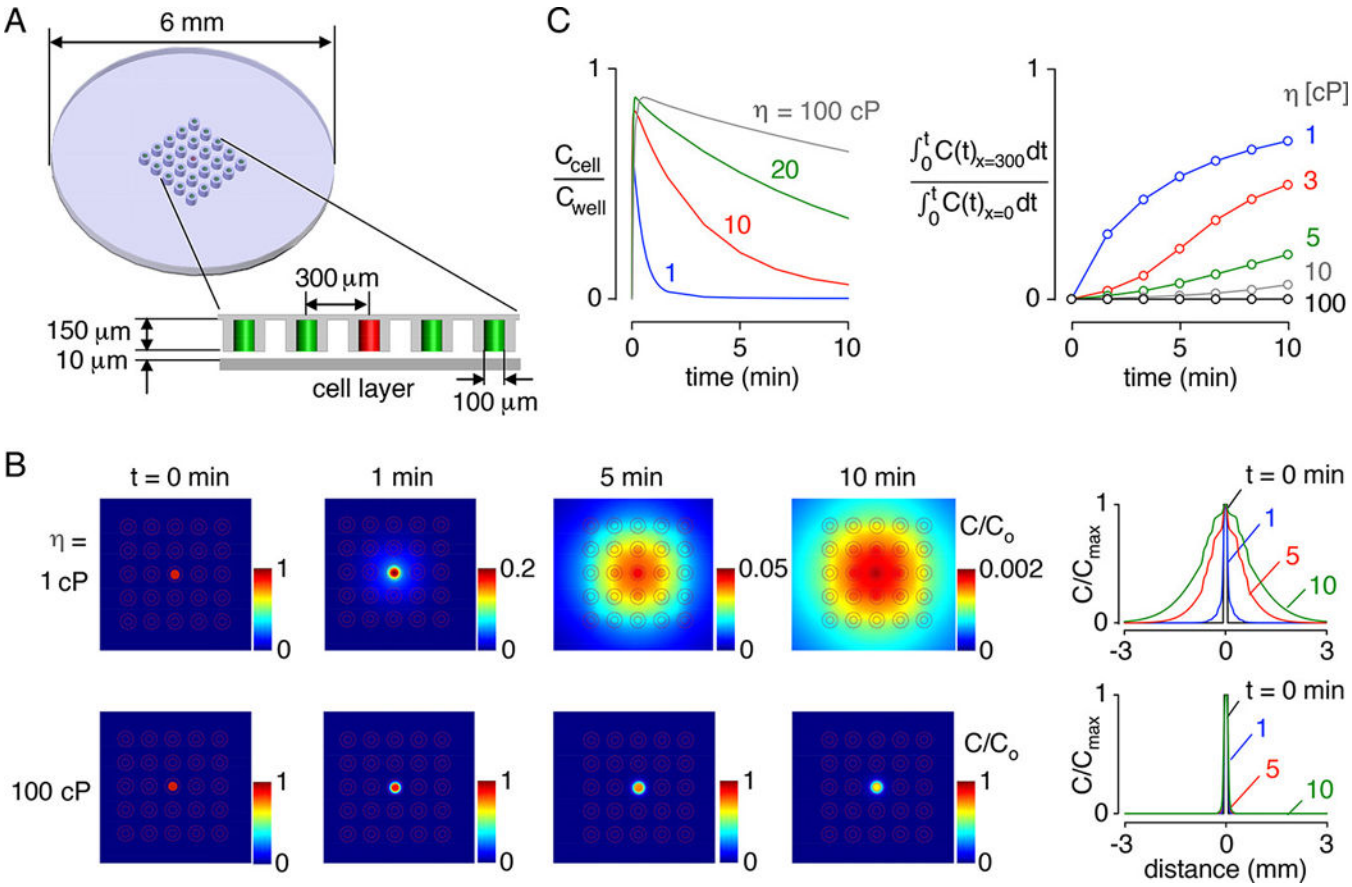


**Figure 2.**

Computational modeling of cell exposure to compounds released from hollow micropillars. (A) Modeled 5 × 5 hollow micropillar array with indicated geometry. (B) Initial condition: compound was uniformly distributed throughout the cylindrical volume of the central hollow micropillar, with zero concentration elsewhere. Compound concentration profiles at the cell surface shown as pseudo-colored two-dimensional images (left) and as intensity line scans through the center of the central micropillar (right). Concentration profiles shown at different times after addition of solutions with relative viscosity ($\eta$) of 1 cP (top) and 100 cP (bottom). (C) Compound exposure to cells overlying the central micropillar well. (left) Time course of compound exposure for indicated $\eta$ of overlying solution. (right) Cross-talk from neighboring wells quantified as time-integrated compound exposure in neighboring well normalized to central well.

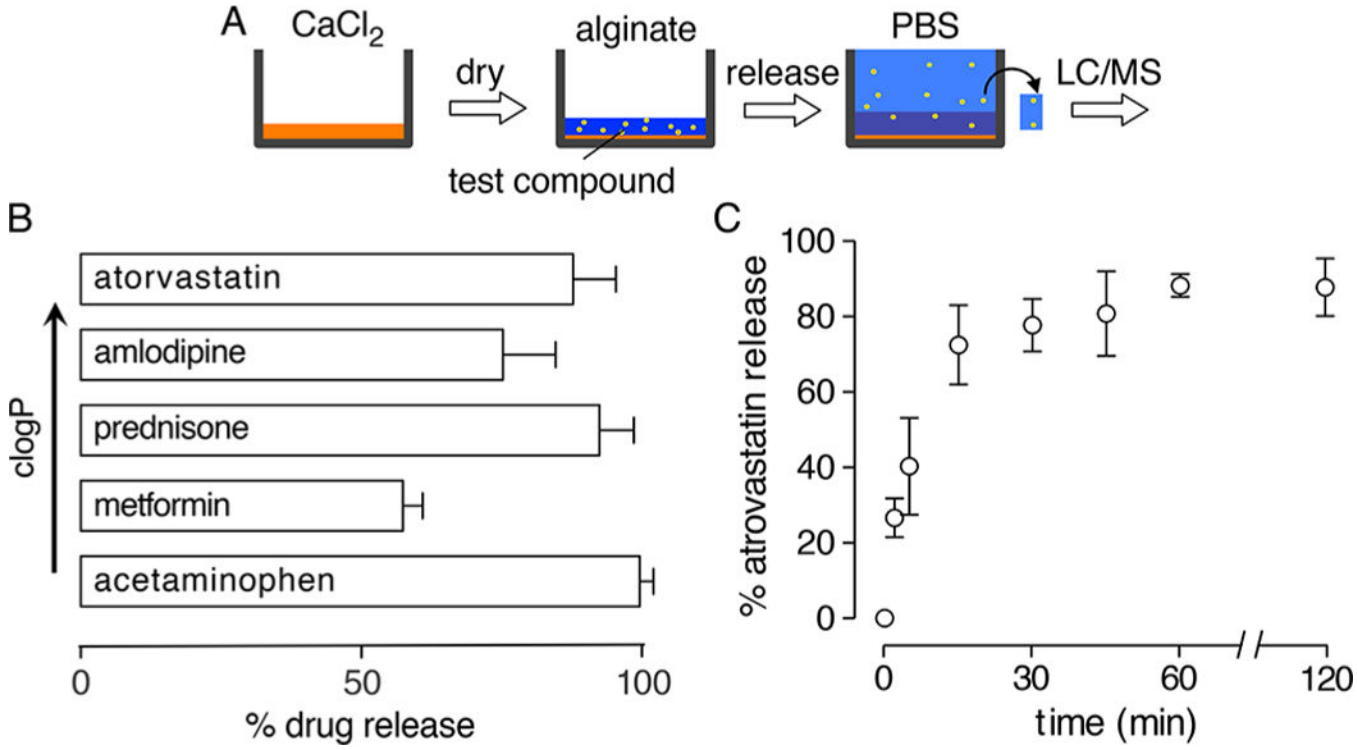


**Figure 3.**

Drug release from alginate hydrogel. (A) Indicated drugs at 10 $\mu$M were dissolved in alginate hydrogels as described under Methods, and after gelation, the hydrogel was covered with PBS at time zero. (B) Drug release was quantified by LC/MS at 3 h (mean ± S.E.M., $n$ = 3). (C) Kinetics of atrovastatin release from hydrogel (mean ± S.E.M., $n$ = 3).

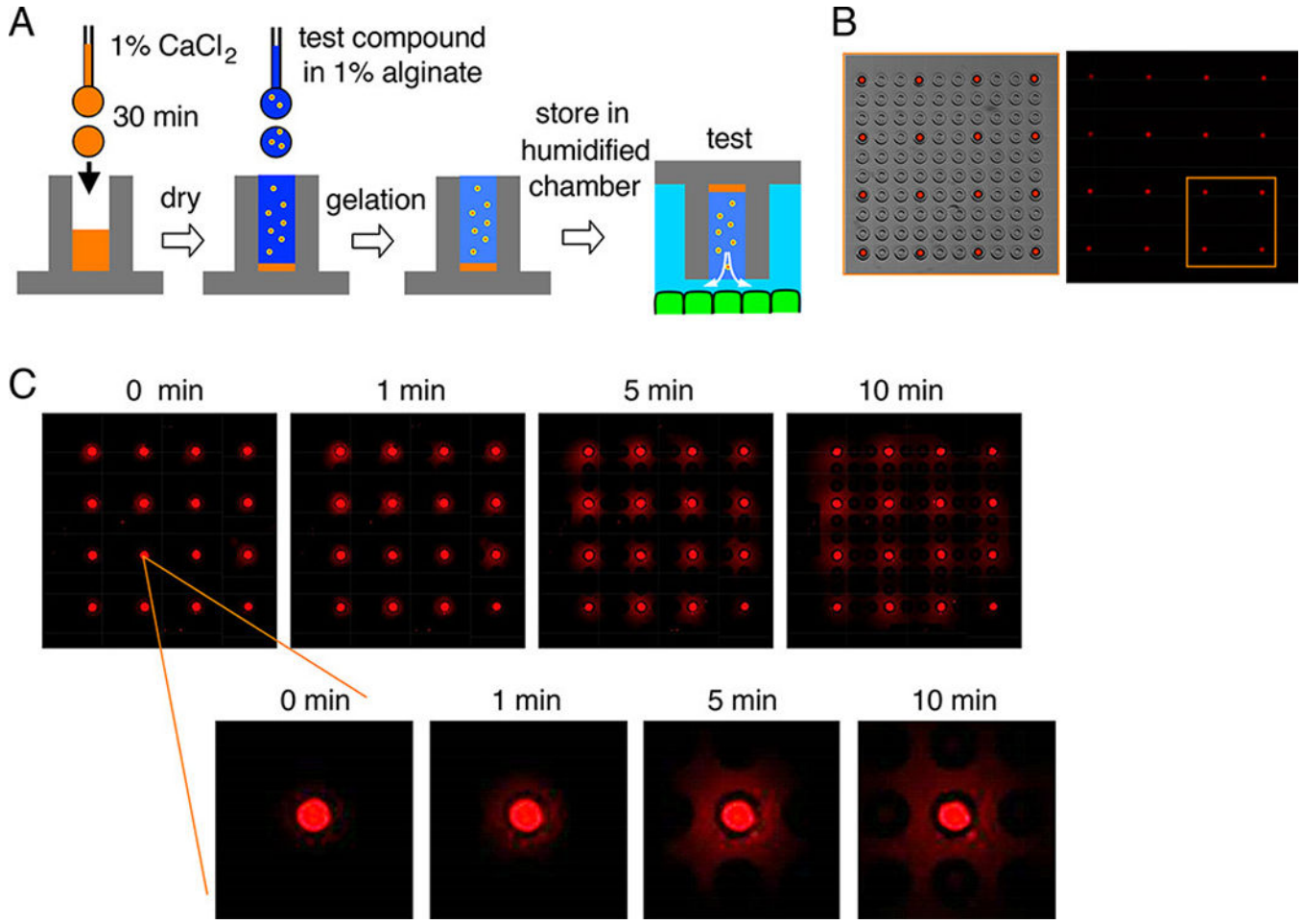


**Figure 4.**

Release and diffusion of fluorescent dye from hollow micropillars. (A) Hollow micropillars were dispensed with alginate containing rhodamine 101. (B) Rhodamine 101 was added to a subset of micropillars as shown schematically (left) and by fluorescence microscopy (right). (C) Rhodamine 101 fluorescence images at indicated times after contacting a cell layer with a solution of relative viscosity of 100 cP.

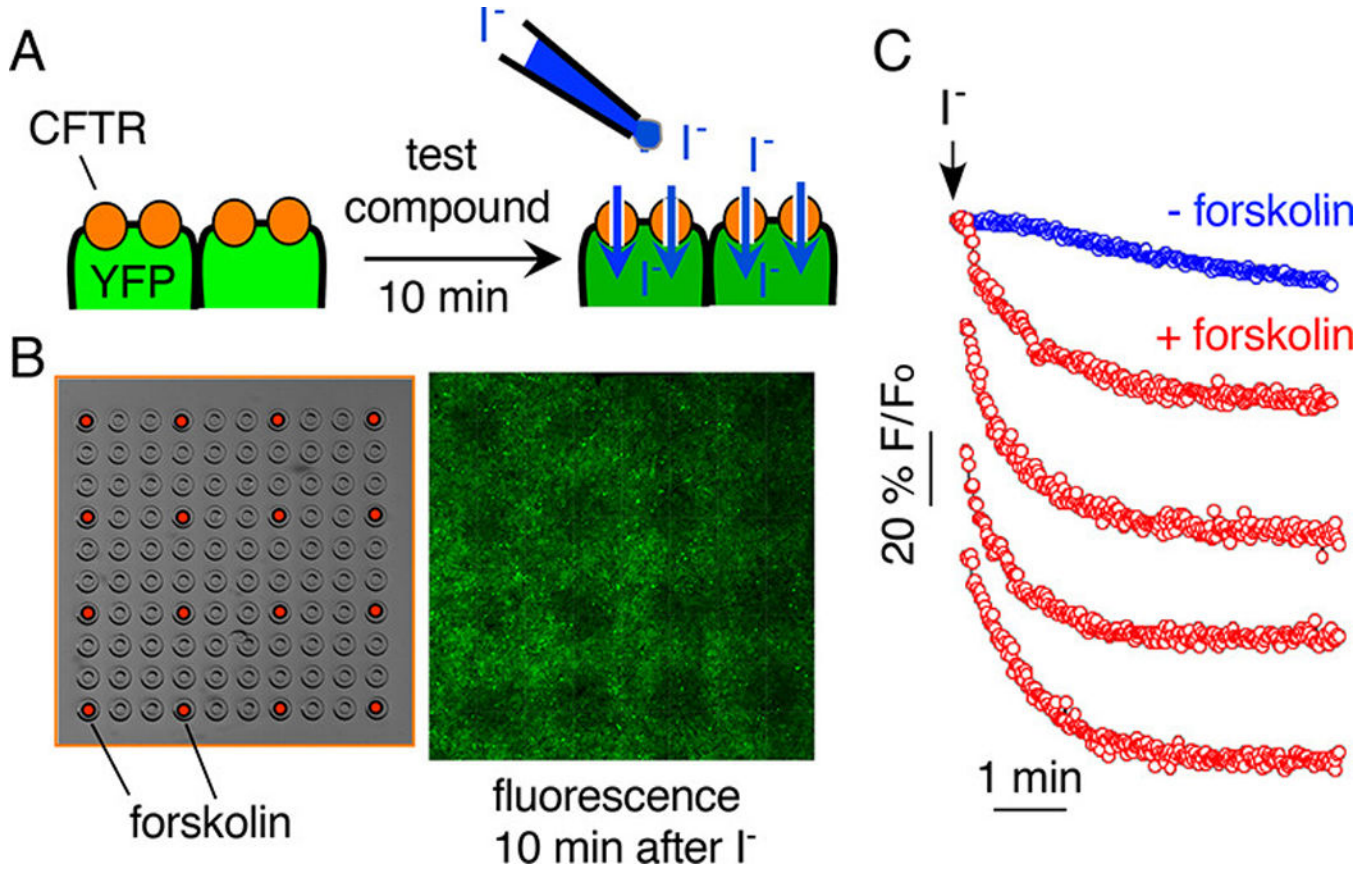


**Figure 5.**

CFTR activator assay done using hollow micropillar array. (A) CFTR-mediated $I^-$ influx was measured in FRT epithelial cells expressing CFTR and a YFP halide-sensing protein from the kinetics of YFP fluorescence quenching following addition of $I^-$ to the extracellular solution. (B) A 10 × 10 hollow micropillar array containing 10 $\mu$M forksolin in a subset of micropillar wells (left, red colored wells) was contacted with the FRT cell layer cultured on a porous support for 10 min prior to addition of $I^-$ and full-field fluorescence imaging. YFP fluorescence image at 10 min after $I^-$ addition (right). (C) Deduced kinetics of YFP fluorescence quenching from cells overlying micropillars without forskolin ("−forskolin") and four examples of micropillars with forskolin ("+forskolin").